ELSEVIER

Journal of Photochemistry and Photobiology A: Chemistry 145 (2001) 229–236

Journal of Photochemistry and Photobiology A:Chemistry

www.elsevier.com/locate/jphotochem

A comparative examination of photoproducts formed in the 248 and 193 nm ablation of doped PMMA

A. Athanassiou [a,*], E. Andreou [a], D. Fragouli [a], D. Anglos [a], S. Georgiou [a], C. Fotakis [b]

[a] *Foundation for Research and Technology-Hellas, Institute of Electronic Structure and Laser, P.O. Box 1527, 71110 Heraklion, Crete, Greece*
[b] *Department of Physics, University of Crete , Heraklion, Crete, Greece*

Abstract

A comparative examination of the photoproducts formed in the 193 and 248 nm ablation of PMMA doped with the highly photodissociable iodo-naphthalene is presented. To this end, laser-induced fluorescence is employed to probe the dopant-derived emitting photoproducts that remain in the substrate following ablation. It is found that the emitting products formed at these two wavelengths are qualitatively the same. However, the dependence of the amount of the photoproduct remaining in the substrate on laser fluence differs. In the case of the ablation at 248 nm, there is a sharp increase in the photoproduct amount, whereas in the ablation at 193 nm, the remaining photoproduct quantity is smaller than that expected on the basis of the linear dependence observed at lower fluences. Plausible explanations for these differences are advanced. © 2001 Elsevier Science B.V. All rights reserved.

Keywords: UV ablation; Doped PMMA; Photochemistry; Photoproducts

1. Introduction

Ultraviolet laser ablation has provided the basis for important techniques aiming at the analysis and the processing of molecular solids. These techniques have found use in a wide range of fields, such as microelectronics (microlithography [1], polymer processing [2,3]), telecommunications (index modulation in optical fibre cores [4]), medicine (angioplasty, photorefractive keratectomy [5], treatment of tumours in the eye [6]), and art conservation (laser restoration of painted artworks [7,8]). In these applications, UV ablation is employed for effecting clean material removal, with preferably minimal, if any, side effects to the substrate that may compromise its integrity. However, for effective material removal, relatively high-intensity UV laser pulses have to be employed to irradiate molecular/organic substrates that include a wide variety of chromophores. Several of the included chromophores are photosensitive, dissociating into highly reactive fragments upon photoexcitation. As a result, an amount of photoproducts is expected to remain in the irradiated substrate after the etching process. Thus, minimisation of the photomodifications in the remaining substrate is crucial for the success and the optimisation of UV laser processing schemes.

Despite extensive work, a full characterisation and understanding of the parameters that affect photochemical modifications/effects in the UV laser ablation of molecular substrates has yet to be achieved. A large number of basic studies have been performed, but they focus mainly on elucidating the extent to which photochemical processes contribute to the material ejection (i.e., if a photochemical mechanism is responsible for ablation), rather than on the parameter dependence of the finally induced photochemical modifications. On the other hand, it is clear that a full characterisation of these effects and of their dependence on laser-processing parameters is difficult to be achieved in the chemically complex substrates encountered in the above applications (i.e., painted artworks, tissue, etc.).

For addressing the above problem, we have turned to the study of the UV ablation of systems consisting of polymers doped with small photosensitive organic compounds such as halonaphthalenes. On one hand, these systems constitute a good model for the substrates encountered in the various applications of UV ablation. For instance, they present close analogies to the painting medium in artworks, where pigments are dispersed within an organic polymerised medium, and to the tissues that include a variety of proteins and other biological chromophores within the collagen layer (stroma). On the other hand, as compared with these substrates, the model systems offer the advantage that the modifications of the dopants can be probed in detail. Thus, they enable a systematic characterisation of the role of the

* Corresponding author. Tel.: +30-81-391-382; fax: +30-81-391-318.
E-mail address: nassia@iesl.forth.gr (A. Athanassiou).

1010-6030/01/$ – see front matter © 2001 Elsevier Science B.V. All rights reserved.
PII: S1010-6030(01)00587-1

various laser-processing parameters in determining the degree of the induced chemical modifications. Furthermore, the well-known photochemistry of these dopants provides a basis for the elucidation and understanding of the factors responsible for this influence.

The potential of probing dopant dynamics has been nicely illustrated by Masuhara and co-workers [9–11] in the examination of the nature of the absorption processes in the UV ablation of polymers. A number of interesting photophysical processes have been shown to occur, including cyclic multiphotonic processes, efficient electronic energy transfer processes, etc. In particular of direct relevance to the present study was the examination of the laser ablation dynamics of PMMA films doped with 5-diano Meldrum's acid. By using transient absorption spectroscopy, they were able to monitor the photodecomposition of the precursor. The photodecomposition yield was determined to be somewhat smaller than unity, with a major percentage of the ketene photoproduct of the photodecomposition appearing within the laser pulse and a minor percentage appearing on later times (presumably formed through thermal decomposition). The important conclusion of the work was that ablation is governed by the amount of the absorbed energy, despite the high quantum yield photodecomposion of the precursor. This energy deposition is indicated to be attained via repeated photon absorption by the ketene photoproduct. Another study relevant to the present work is the decomposition of the photosensitive dopant, diazirine, within PMMA films in the irradiation with 266 nm, 60 ps pulses [12]. By using picosecond infrared spectroscopy, the intensity of the ketoketene intermediate was followed with nanosecond time resolution both below and above the threshold. No significant change was found in the signal intensity over the examined fluence range, consistent with a one-photon process and a near-unity quantum yield of decomposition. In another study [13], time-resolved absorption spectroscopy was employed to follow the decomposition of the 1,1,3,5-tetraphenylacetone dopant within PMMA matrix upon excitation at 266 nm. It was suggested that one-, two- and three-photon processes are important in the decomposition of the precursors. Nevertheless, despite the increasing contribution of multiphoton processes, no major differences in the reaction intermediates were observed as the ablation threshold is reached.

In close analogy to the previous studies, we have examined previously the photoproducts formed in the ablation of NapX (X = Br, I)-doped poly(methylmethacrylate) (PMMA) films at 248 nm. Laser-induced fluorescence was employed for monitoring the emitting photoproducts that remain in the substrate following ablation. Photoproduct probing was performed on relatively long time scales (seconds to minutes) after the laser ablation pulse, so as to ensure that all bulk reactions have been completed and formation of photoproducts is complete. Naphthalene-substituted derivatives were observed to be the major emitting photoproducts in the ablation of weakly doped films, whereas in the irradiation of films with a somewhat higher dopant concentration (>1% by weight), Nap_2-type species were also evidenced. On the basis of the solution chemistry of the compounds, the particular dopants undergo a simple homolytic dissociation to Nap radicals and iodine atom [14,15]. The Nap radicals formed upon photodissociation of the dopants abstract a hydrogen atom or other small units from the PMMA side groups to form NapH-like photoproducts. Given the very short lifetime of the excited states of the iodoaromatics (0.9 ps for iodonaphthalene) [15], photoproduct formation through direct reactions of the excited states can be ruled out. The efficient formation of Nap_2-type products that is observed for higher dopant concentrations was ascribed to the high mobility of the produced radicals within a highly disrupted by the UV ablation polymer lattice [16].

This study extends the previous work into the comparative examination of the photochemical modifications effected in the ablation of doped PMMA at 248 and 193 nm. The photoproduct formation is studied both qualitatively, i.e., characterisation of their nature, and quantitatively, i.e., fluence dependence of their formation and accumulation in the substrate. Qualitatively, the products, at least the emitting ones, are found to be the same independently of the wavelength of the ablating laser pulse. However, the fluence dependence of the photoproduct amount that remains in the substrate following ablation is found to differ considerably at the two wavelengths. These results are discussed for their mechanistic significance as well as for their implications concerning optimisation of UV laser processing of molecular/organic substrates.

2. Experimental

2.1. Samples

Highly purified PMMA ($M_w \sim 120\,000$) are doped with the iodo-derivative of the aromatic naphthalene (NapI) (Aldrich). For the preparation of the films, solutions of the purified polymer and the dopant in dichloromethane (CH_2Cl_2), the solutions are cast on quartz substrates. The samples were subsequently dried for several hours, first in air and then under vacuum. The dopant concentration varies from 0.1 to 4.0 wt.% and the typical film thickness is in the range 10–50 μm, as measured by a profilemeter.

2.2. Experimental arrangement

The experiments are performed with a nanosecond KrF and ArF excimer laser (Lambda-Physik EMG150) operating at 248 and 193 nm, respectively. The laser beam is focused perpendicularly onto the sample in a rectangular spot of 6–10 mm^2, using a quartz spherical lens ($f = +500$ mm). Irradiation of the samples is performed in ambient atmosphere. Pump pulses of varying fluence values irradiate the doped polymer films at a virgin region each time. In all cases, photoproduct fluorescence is induced by excitation

with 248 nm laser pulses of very low fluence ($F_{laser} \leq 3\,mJ\,cm^{-2}$). Thus, photoproduct formation by the probe beam itself is negligible and the recorded fluorescence can be assumed to derive exclusively from photoproducts formed by the previous "pump" pulse. In the experiments in which ablation is effected with 248 nm, ablation and probing are effected with the same beam configuration (except for the decreased fluence of the probe beam) and thus the probing/excitation is performed on exactly the ablated area. For the experiments in which the ablation is performed at 193 nm, the 248 nm probing beam is focused in an area closely matched to the ablated area. However, as the overlap of the probed and the ablated area is not perfect, the fluorescence intensities recorded for samples irradiated at the two wavelengths are not exactly comparable (i.e., they have not been normalised), although the error is expected to be small.

A relatively long delay (of the order of several seconds) between the pump and probe pulses is employed for ensuring nearly quantitative reaction of the photo-induced radicals and formation of stable photoproducts. Indeed, the photoproduct fluorescence intensity remains constant for longer delay times.

The emission induced by the probe beam is collected by an optical fibre oriented nearly perpendicular to the sample and at a distance of 1–2 cm away from its surface. An *x–y* micrometer ensures accurate positioning of the optical fibre relatively to the irradiated spot. The light from the fibre is spectrally analysed in a 0.20 m grating spectrograph equipped with a 300 grooves/mm grating, which provides an effective spectral window of 280 nm at the exit port of the spectrograph. The emission spectrum is recorded on an optical multichannel analyser based on an intensified photodiode array detector (OMA III system, EG&G PARC Model 1406). A computer interface system is finally used for the storage and analysis of the recorded spectra.

3. Results and discussion

3.1. Spectral photoproduct examination

Fig. 1 exhibits the fluorescence probe spectra recorded from 0.4 wt.% NapI/PMMA film after irradiation 193 and 248 nm, at a fluence value just above the corresponding ablation thresholds ($\sim$500 mJ cm^{-2} at 248 nm and $\sim$95 mJ cm^{-2} at 193 nm, as established independently by profilometric measurements). The spectra in the figure represent the spectrally resolved emission induced by the 248 nm probing, after irradiation of the substrates with a single "pump" pulse at the indicated wavelength. In both cases, probe fluorescence excitation is effected at 248 nm.

In both cases, the probe spectra recorded from the ablated NapI-doped polymers are dominated by an emission band between 320 and 340 nm. As mentioned before, due to its very rapid dissociation, the NapI precursor is characterised by negligible fluorescence. Furthermore, the indicated band does not appear in the corresponding irradiation of neat PMMA film. Therefore, this emission band is due to emitting photoproducts produced by the iodoaromatic dopants. The band can be ascribed to the $^1B_{3u} \rightarrow {}^1A_{1g}$ transition characteristic of NapH compound. This assignment is supported by the comparison with spectra recorded, under the present experimental conditions, for NapH/PMMA films (an indicative one for a 0.1 wt.% dopant concentration is included in Fig. 1 for comparison reasons). However, the aforementioned emission band is not sensitive to the substitution of

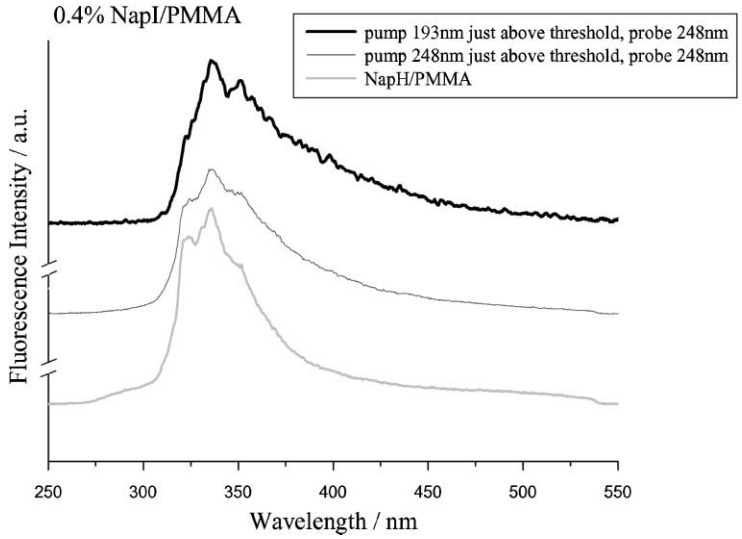

Fig. 1. Photoproduct fluorescence spectra recorded from 0.4 wt.% NapI/PMMA films after irradiation with a single pulse at 193 and 248 nm, and fluence values just above the corresponding ablation thresholds. In all cases, photoproduct emission is induced by excitation at 248 nm. For comparison purposes, a spectrum recorded from PMMA doped with NapH (0.1 wt.%) is also included.

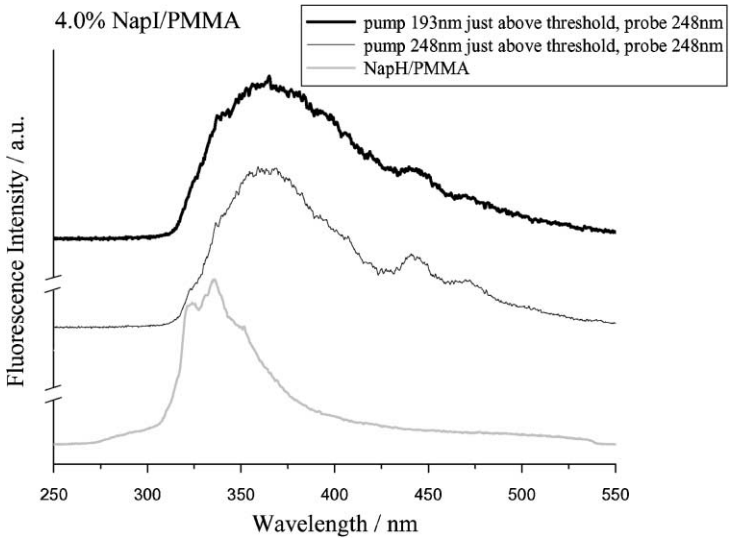

Fig. 2. Photoproduct fluorescence spectra recorded from 4.0 wt.% NapI/PMMA film after irradiation with a single pulse 193 and 248 nm, and fluence values just above the corresponding ablation thresholds. In all cases, photoproduct emission is induced by excitation at 248 nm.

the aromatic skeleton and thus it is not possible to ascertain the exact nature of the products only from the fluorescence spectra. Consequently, the photoproducts that fluoresce at the specific wavelengths will be referred to as NapH-like.

The examination of Fig. 1 makes it clear that the photoproduct emission spectra are nearly the same independently of the ablation wavelength. In both cases, the dominant photoproducts are NapH-like compounds. Preliminary examination indicates equal temporal decays of the fluorescence, within experimental error, for samples irradiated at either wavelength, thereby confirming that the same type of naphthalene derivative is formed in both cases.

Fig. 2 illustrates the laser-induced fluorescence spectra recorded after irradiation of a NapI-doped PMMA system with a dopant concentration 10 times larger than in the previous case (4.0 wt.% NapI). In this case too, the samples have been irradiated with only one pump (ablating) pulse at a fluence value just above the corresponding ablation thresholds values ($\approx$200 mJ cm^{-2} at 248 nm and $\approx$80 mJ cm^{-2} at 193 nm). For these samples, the photoproduct spectra are much broader than the ones recorded from the 0.4 wt.% samples, and additionally a well-defined double peak structure is evident around 450 nm. Both the spectral broadening and the double-peak feature become more intense with increasing laser fluence. In fact, the intensity in the 350–400 nm range is so pronounced that the NapH-like photoproduct emission between 320 and 340 nm is hardly discernible.

Bi-polycyclic aromatic hydrocarbons are known to exhibit a fairly broad emission band at longer wavelengths than the emission band of their polycyclic aromatic hydrocarbons counterparts [17]. Therefore, the spectral broadening is consistent with Nap_2 species, whereas the double peak feature may be possibly ascribed to Nap_2X species, where X is some intermediate chain deriving from the decomposition of the PMMA. In particular, the photolysis of highly concentrated solutions of NapI in inactive solvents (i.e., C_6H_6), under the present conditions, results in spectra dominated by a band at 370 nm, in very good correspondence with the broadening observed in the above spectra. Furthermore, the intensity of the long wavelength emission ($\lambda \geq 350$ nm) grows supralinearly with increasing NapX (X = Br, I) concentration, consistent with a bimolecular process. In fact, this broadening is also indicated for the 0.4 wt.% doped samples, as a closer examination of Fig. 1 shows.

The important point for the present purpose is that even for films of a much higher dopant concentration, where evidently additional reactivity pathways become important, no particular qualitative difference is observed following ablation at either wavelength. Aside from a small change in the relative yields of the Nap_2-type versus NapH-type photoproducts, the photoproduct emissions recorded from the NapI-doped PMMA films after ablation are remarkably similar. This observation indicates that the same reactivity pathways and processes must operate in the ablation at both wavelengths. However, at present, the "dark", non-fluorescing products have not been identified and characterised. As a result, the validity of the previous statement cannot be yet generalised.

3.2. F_{laser}-dependence of NapH photoproduct formation

In contrast to the qualitative examination, differences are observed between the two wavelengths in the quantitative examination of the dependence of the photoproduct formation and accumulation in the film. To this end, Figs. 3 and 4 present the dependence of the fluorescence intensity (measured at 337 nm) of the NapH-like product after a single pump pulse for the 0.4 wt.% NapI–PMMA system at 248 and 193 nm, respectively. This intensity reflects essentially the amount of the fluorescing naphthyl species that remain

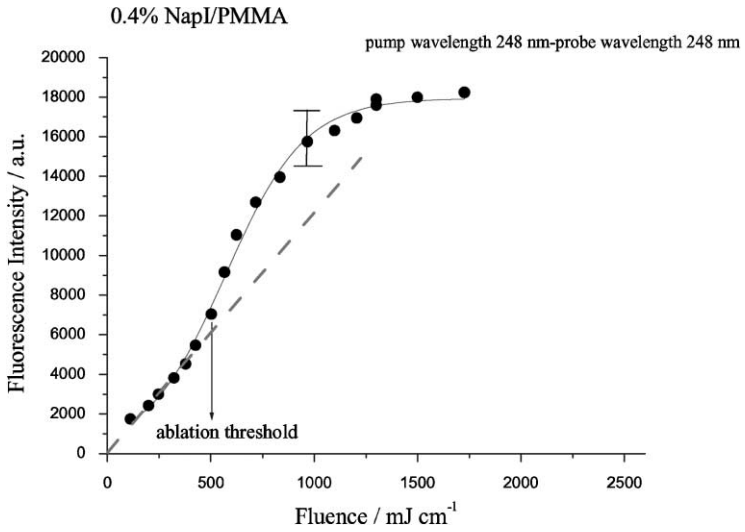

Fig. 3. Fluorescence intensity of the NapH-like photoproduct ($\lambda = 337$ nm) remaining in the substrate, following irradiation at 248 nm. The error bars represent 2σ as determined from at least five different measurements. The main source of error is thought to be the variation in film thickness at the probed points.

in the substrate after irradiation with the "pump" pulse. The photoproduct intensities following irradiation at 193 nm are lower than the corresponding ones following irradiation at 248 nm, although as described in Section 2, the fluorescence intensities recorded for samples irradiated at the two wavelengths are not normalised.

For doping with 0.4 wt.% NapI and the film thickness employed herein, the samples can be considered to be approximately in the optically thin limit (absorbances being 0.3–0.4 at the 248 nm probing wavelength). Therefore, for irradiation at low "pump" laser fluences, the fluorescence values can be considered to be exactly proportional to the photoproduct formed in the substrate, without the need for "inner-filter" (self-absorption) effect corrections. In contrast, the fluorescence intensities recorded from samples irradiated above the threshold cannot be directly correlated with the photoproduct quantity due to the influence of scattering effects on the probing/fluorescence step. Ablation results in a highly irregular film morphology, with a consequent modification in the propagation of the probing beam and in the intensity of the induced fluorescence. We have described elsewhere [18] the different approaches employed for ensuring that the observed changes above the ablation threshold are not due to the influence of these scattering effects. However, despite several different approaches, a methodology for the extraction of reliable quantitative information from highly scattering media has yet to be attained in the literature. In view of this, we do not try to derive quantitative

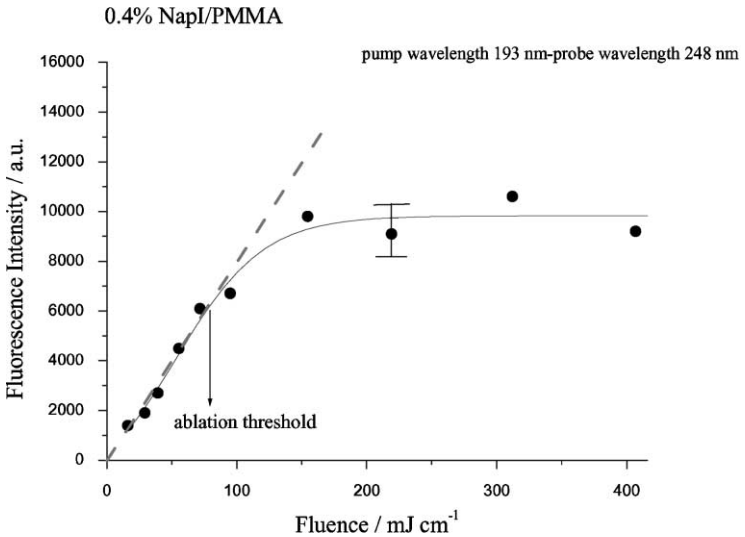

Fig. 4. Fluorescence intensity of the NapH-like photoproduct ($\lambda = 337$ nm) remaining in the substrate, following irradiation at 193 nm.

information, but instead concentrate on the different F_{laser} dependences observed at the two wavelengths.

At both wavelengths, the photoproduct-fluorescence intensity increases smoothly with laser fluence at low fluences. A log–log examination of the signal establishes the increase to be linear (1.1 ± 0.3 from five measurements for each "pump" wavelength). The result is consistent with a one-photon dissociation of the photosensitive dopants at these low fluences and formation of the NapH-type photoproducts via subsequent abstraction reactions of the Nap produced radical. However, significant deviations from this linear dependence are observed for fluences above the threshold. The dotted line in the two figures represents the extrapolation of the dependence of the photoproduct intensity that is observed at low fluences to fluences above the ablation threshold. It is clear that the F_{laser} dependence of photoproduct formation above the threshold changes from that at low fluences in a different manner at the two employed wavelengths.

For irradiation at 248 nm, there is an abrupt change in the slope $\sim$500 mJ cm^{-2}, and the photoproduct fluorescence starts increasing sharply with increasing laser fluence. Consequently, the ablation process appears to result in a significant enhancement of the amount of photoproducts remaining in the substrate. The fluorescence intensity increases until, at high fluences, it finally reaches a plateau indicative of nearly quantitative photodegradation of the chromophores within the probed volume. In contrast, in the case of 193 nm, the fluorescence intensity reaches a plateau at fluence just above the ablation threshold. Thus, in the ablation at 193 nm, the photoproduct quantity that remains in the substrate is nearly constant and independent of the employed laser fluence. Furthermore, the quantity of photoproducts that remain in the substrate is found to be decreased compared to the hypothetical case of linear behaviour.

In all, the study provides unexpected results concerning the photochemical modifications effected in the ablation of NapI–PMMA-doped films at the two wavelengths. On one hand, as far as the nature of (emitting) photoproducts is concerned, no particular difference is observed between the two wavelengths. On the other, the F_{laser} dependence of the photoproduct that remains in the substrate differs in a striking way.

Concerning the qualitative aspect of the comparison, the spectral similarity in Figs. 1 and 2 indicates that the nature of the induced photoproducts upon ablation does not change at 193 and 248 nm. In this respect, particularly important indication is thought to be the comparable Nap_2-type photoproduct formation indicated for the samples with high dopant concentration. As discussed elsewhere [16,18], the observation of Nap_2-type products strongly indicates a very high mobility of the Nap radicals in the UV ablation of polymers. Alternative pathways (such as direct formation of these products via reactions of excited states or within excimers) are not consistent with the experimental observations [16].

If Nap_2-type photoproducts are formed via reactions of diffusing Nap radicals, then radical mobility within the polymer matrix during ablation must be very high. Even at the highest concentration (4 wt.%), the average distance between dopant molecules is $\sim$19 Å. Assuming the mobility to be described by the usual diffusion law, $r = (2Dt)^{0.5}$, it follows that D must be at least $\sim 5 \times 10^{-8}$ cm^2 s^{-1} for formation of Nap_2 on microsecond time scale and $\sim 5 \times 10^{-11}$ cm^2 s^{-1} for formation on milisecond time scale. These values are too high for diffusion of such molecules within a glassy polymer matrix, where values of $<10^{-13}$ cm^2 s^{-1} are generally reported for this molecular size [19]. In fact, the slight observation of Nap_2-type emission for dopant concentration as low as 0.4 wt.% indicates that D values may be even an order of magnitude higher than indicated. This conclusion for very high mobility closely correlates with the finding that singlet–singlet and triplet–triplet energy transfer processes are highly enhanced during UV ablation [11]. This observation also presupposes, to some extent, a high degree of mobility of the excited chromophores. The high mobility suggests that the lattice structure of the polymer is highly disrupted in UV ablation. Within the framework of this hypothesis, then, the spectral similarity indicated in Figs. 1 and 2 suggests that the structure of the PMMA is comparably modified upon ablation at both irradiation wavelengths, 248 and 193 nm. Thus, contrary to previous suggestions [20,21], there is no evidence, at least, in the present work of a qualitatively different mechanism at the two wavelengths. Our present results do not provide direct information about the nature of the mechanisms, but qualitatively they are consistent with a photothermal mechanism.

The previous conclusion about the similarity of the processes at the two wavelengths, however, raises difficulties in accounting for the different F_{laser}dependences. The similarity of the processes would suggest similar or at least comparable efficiencies for photoproduct formation at the two wavelengths. This is also supported from the known solution chemistry of the studied dopants [14]. Therefore, the difference in the F_{laser} dependence of the photoproduct formation must be ascribed to subtler factors. At this moment, the nature of these factors cannot be confidently ascertained, but at least the following hypotheses can account partially for the observed difference.

First, the difference between the two wavelengths may be partly due to a less effective light absorption by the ejected plume at 248 nm than at 193 nm. In the case of 248 nm, the plateau observed at high fluences corresponds well to the plateau in the etching curve as a function of F_{laser}. This plateau has been generally ascribed to the efficient screening of the plume (i.e., absorption or scattering of some of the incident light by the dense cloud of the ejected fragments), as well as to the scattering of the laser light by bubbles etc. developed within the substrate [2,9–13]. Evidently, the same factors will also affect the efficiency of photolysis and photoproduct formation, thereby accounting for the plateau in

Table 1
Approximate ratios of the etch depth close to the ablation threshold over the penetration depth for PMMA at 193 and 248 nm[a]

Wavelength (nm)	Etch depth[b] (cm)	Penetration depth (cm)	Etch depth (penetration depth)$^{-1}$
193	0.15×10^{-4} [20][c]	2.08×10^{-4} [22]	0.06
	0.10×10^{-4} [21][c]	2.22×10^{-4} [23]	
248	0.8×10^{-4} [23,24][d]	0.98×10^{-2} [24]	0.008

[a] The etch depth and penetration depth values have been collected from the literature.
[b] Reported values represent etch depth at a fluence close to the corresponding ablation thresholds.
[c] Etching depth at ~100 mJ cm^{-1}.
[d] Etching depth at ~800 mJ cm^{-1}.

Fig. 3. An analogous explanation could be advanced for the observation of a plateau in Fig. 4, although the comparison with the published etching curves (for neat PMMA) does not show a full correspondence. We are currently performing LIBS measurements as a function of laser fluence for a more direct assessment of the importance of this factor at the two wavelengths.

Another factor that contributes to the observed differences in the F_{laser} dependences at the two wavelengths can be provided by consideration of the relative etching depth versus the optical penetration depth at the two wavelengths. Since above the threshold, the recorded fluorescence represents the total amount of formed photoproduct minus the amount removed by the etching, the plateau observed in the case of 193 nm may be explained by the efficient product removal. In contrast, at 248 nm, the doped PMMA system is a much weaker absorber than at 193 nm. Indeed, the ratio of the etch depth of PMMA close to the ablation threshold over the light penetration depth is one order of magnitude larger in the case of irradiation at 193 nm than that in the case of irradiation at 248 nm, as shown in Table 1 based on literature values for neat PMMA. The comparison clearly indicates that etching at 193 nm is much more efficient in removing any photoproducts. With increasing laser fluence, the increase in the formed photoproduct is counter-balanced by the higher amount (depth) of film removed, thereby accounting for the nearly constant quantity of photoproduct remaining in the substrate. In contrast, at 248 nm, the increase in the etching depth is not sufficient to counter-balance the increased photoproduct formation within the long optical penetration depth.

The previous argument relies on the assumption of one-photon absorption coefficients. As shown by Masuhara et al., in the UV ablation of polymers, multiphoton processes become highly efficient through the proposed cyclic multiphotonic process. Thus, the effective absorption coefficient differs significantly from the low-fluence linear one and so a comparison of the depths of photoproduct formation based on the linear absorption coefficients may not be valid. Nevertheless, it is likely that multiphoton processes are much more probable for the studied system at 193 nm than at 248 nm, and the previous argument for the different F_{laser} dependences of formed photoproduct still holds.

The operation of multiphoton processes and of efficient energy transfer processes in the ablation of doped polymers may also affect the degree of photolysis of the incorporated dopants. For instance, electronic energy transfer to NapI molecules may result in decomposition of dopants in addition to the directly photodissociated ones. Thus, variations in these processes at the two wavelengths may be partly responsible for the different F_{laser} dependences.

Alternatively, we have proposed that the observed increase may be due to the reduced importance of "cage effects" above the ablation threshold. Generally, photolysis efficiency of chromophores in polymers is reduced from that in solution due to the constraining environment of the polymer, the so-called "cage effects". As a result, a large number of photoexcited molecules below threshold do not produce "free" radicals that can subsequently react to form new products. However, as argued above, under conditions of ablation, the integrity of the substrate is severely compromised. Consequently, the radicals Nap and I can be expected to have a much higher possibility of escaping rather than recombining, thereby resulting in a much more efficient photoproduct formation. This hypothesis can thus explain why photoproduct formation increases above threshold in the case of irradiation at 248 nm. In the case of the 193 nm ablation, this increase is not observed because, as suggested above, it is balanced by the material removal.

4. Summary and conclusions

An examination of the different photochemical modifications that occur in the UV ablation of NapI-doped PMMA at 248 and 193 nm is presented, using laser-induced fluorescence technique for the probing the photoproducts. The NapI dopant has nearly zero fluorescence quantum efficiency, while its photoproducts fluoresce strongly and therefore can be used as sensitive indicators of the photolysis yield of the parent molecule. It is demonstrated that the nature of the induced photoproducts upon ablation does not change when two different UV wavelengths of 193 and 248 nm are used. Therefore, the reactivity patterns that occur upon ablation at these two wavelengths appear to be the same.

In contrast to this similarity in the formation of photoproducts, the F_{laser} dependences of the photoproducts remaining in the substrate differ remarkably in the two cases. In the case of the weakly absorbed 248 nm, the remaining photoproducts exhibit a sharp increase after the ablation threshold is exceeded. On the contrary, for the strongly absorbed 193 nm irradiation, the intensity of the residual photoproducts reaches a plateau closely above the ablation threshold. Various possibilities have been considered to account for the observed difference, with a most likely one appearing to be the much higher effective absorption coefficient at 193 nm.

As far as we know, this is the first, albeit semi-quantitative, determination of the full F_{laser} dependence of photoproduct formation in the substrate in the UV ablation at the two wavelengths. Independent of the responsible mechanisms for the observed dependence, the study clearly indicates the importance of careful examination of laser material-processing parameters for effective minimisation of the induced photochemical modifications. In particular, the study suggests that a high absorption coefficient of the substrate ensures a high degree of "photochemical protection" to the remaining material. This indication may explain the effectiveness of UV laser ablation in the processing of highly absorbing molecular/organic substrates. Indeed, in most applications, the incident photons are strongly absorbed by the treated substrate. Thus, the induced photochemical modifications may be better described by the curve of Fig. 4, i.e., they are highly reduced from that expected on the basis of the linear photochemistry that occurs at low laser fluences.

Acknowledgements

The work was supported by the Large Installations Plan DGXII (Project No. G/89100086/GEP) and by the TMR Programme (No. ERB FMRX-CT98-0188) and by PENED administered by the Greek Ministry of Industry.

References

[1] P. Rumsby, E. Harvey, D. Thomas, N. Rizvi, Excimer laser patterning of thick and thin films for high density packaging, SPIE 3184 (1997) 176–185.
[2] D. Bäuerle, Laser Processing and Chemistry, Springer, Berlin, 2000.
[3] J.C. Miller (Ed.), Laser Ablation: Principles and Applications, Springer Series on Material Sciences, Vol. 28, Springer, Berlin, 1994.
[4] W.W. Morey, G.A. Ball, G. Meltz, Photoinduced Bragg Gratings in Optical Fibers, Optics and Photonics News, 1994, pp. 8–14.
[5] S.L. Jacques (Ed.), Laser–Tissue Interaction IX, SPIE Proc. Series 3254, SPIE, Washington, DC, 1998.
[6] P. Hill, Multiphoton excitation eradicates eye cancers, OLE 71 (2000) 29–31.
[7] S. Georgiou, V. Zafiropoulos, D. Anglos, C. Balas, V. Tornari, C. Fotakis, Excimer laser restoration of painted artworks: procedures, mechanisms and effects, Appl. Surf. Sci. 127–129 (1998) 738–745.
[8] S. Georgiou, V. Zafiropoulos, V. Tornari, C. Fotakis, Mechanistic aspects of excimer laser restoration of painted artworks, Laser Phys. 8 (1) (1998) 307–312.
[9] H. Fujiwara, Y. Nakajima, H. Fukumura, H. Masuhara, J. Phys. Chem. 99 (1995) 11481.
[10] H. Fukumura, H. Masuhara, Chem. Phys. Lett. 221 (1994) 373.
[11] H. Furutani, H. Fukumura, H. Masuhara, J. Phys. Chem. 100 (1996) 6871.
[12] T. Lippert, P.O. Stoutland, Appl. Surf. Sci. 109–110 (1997) 43.
[13] B.R. Arnold, J.C. Scaiano, Macromolecules 25 (1992) 1582.
[14] E. Haselbach, Y. Rohner, P. Suppan, Helv. Chim. Acta 73 (1990) 1644.
[15] M. Dzvonik, S. Yang, R. Bersohn, J. Chem. Phys. 61 (11) (1974) 4408.
[16] A. Athanassiou, M. Lassithiotaki, D. Anglos, S. Georgiou, C. Fotakis, Appl. Surf. Sci. 154–155 (2000) 89.
[17] S.A. Tucker, J.M. Griffin, W.E. Acree Jr., M. Zander, R.H. Mitchell, Appl. Spectrosc. 48 (4) (1994) 458.
[18] A. Athanassiou, E. Andreou, D. Anglos, S. Georgiou, C. Fotakis, Appl. Phys. A 69 (7) (1999) S285.
[19] J.E. Mark (Ed.), Physical Properties of Polymers Handbook, American Institute of Physics, Woodbury, NY, 1996.
[20] R. Srinivasan, B. Braren, J. Polym. Sci. 22 (1984) 2601.
[21] E. Sutcliffe, R. Srinivasan, J. Appl. Phys. 60 (9) (1986) 3315.
[22] J. Meyer, J. Kutzner, D. Feldmann, K.H. Welge, Appl. Phys. B 45 (1988) 7.
[23] S.R. Cain, F.C. Burns, C.E. Otis, B. Braren, J. Appl. Phys. 72 (11) (1992) 5172–5178.
[24] S. Küper, M. Stuke, Appl. Phys. B 44 (1987) 199–204.